International Journal of Nanomedicine

Dovepress

open access to scientific and medical research

Open Access Full Text Article

ORIGINAL RESEARCH

Lipopolysaccharide-Preconditioned Dental Follicle Stem Cells Derived Small Extracellular Vesicles Treating Periodontitis via Reactive Oxygen Species/ Mitogen-Activated Protein Kinase Signaling-Mediated Antioxidant Effect

Yanli Huang[1–3], Qian Liu[1,2,4], Li Liu[1,2,4], Fangjun Huo[1,2], Shujuan Guo[1,2,4], Weidong Tian[1,3]

[1]State Key Laboratory of Oral Disease & National Clinical Research Center for Oral Diseases & National Engineering Laboratory for Oral Regenerative Medicine, West China School of Stomatology, Sichuan University, Chengdu, 610041, People's Republic of China; [2]Engineering Research Center of Oral Translational Medicine, Ministry of Education, West China School of Stomatology, Sichuan University, Chengdu, 610041, People's Republic of China; [3]Department of Oral and Maxillofacial Surgery, West China Hospital of Stomatology, Sichuan University, Chengdu, Sichuan, 610041, People's Republic of China; [4]Department of Periodontics, West China School of Stomatology, Sichuan University, Chengdu, Sichuan, 610041, People's Republic of China

Correspondence: Shujuan Guo; Weidong Tian, Tel/Fax +86 028 8550 3499, Email guo_shujuan@126.com; drtwd@sina.com

Purpose: Lipopolysaccharide (LPS) pretreatment can enhance the therapeutic effect of dental follicle stem cells-derived small extracellular vesicles (DFC-sEV) for periodontitis, and this study aimed to investigate the underlying mechanisms and clinical application Of LPS-preconditioned DFC-sEV in periodontitis.

Methods: The protein spectrum of DFC-sEV before and after LPS pretreatment was determined by liquid chromatography-tandem mass spectrometry and bioinformatic analysis. Their effects on inflammatory periodontal ligament stem cells (PDLSCs) and macrophages were investigated for cell proliferation, migration, type 2 macrophage (M2) polarization, and intracellular reactive oxygen species (ROS) levels separately. In addition, the regulation of ROS/Jun amino-terminal kinases (JNK) and ROS/extracellular signal-related kinases (ERK) signaling by LPS-preconditioned DFC-sEV was also studied to reveal the antioxidant mechanism. In vivo, two kinds of DFC-sEV loaded with 0.2% hyaluronic acid (HA) gel were applied for canine periodontitis to evaluate the therapeutic potential.

Results: The proteomic analysis showed that thirty-eight proteins were differentially expressed in LPS-preconditioned DFC-sEV, and interestingly, the highly expressed proteins were mainly involved in antioxidant and enzyme-regulating activities. In addition to promoting PDLSCs and macrophage proliferation, LPS-preconditioned DFC-sEV inhibited intracellular ROS as an antioxidant. It reduced the RANKL/OPG ratio of PDLSCs by inhibiting ROS/JNK signaling under inflammatory conditions and promoted macrophages to polarize toward the M2 phenotype via ROS/ERK signaling. Furthermore, LPS-preconditioned DFC-sEV loaded with the HA injectable system could sustainably release sEV and enhance the therapeutic efficacy for periodontitis in canines.

Conclusion: LPS-preconditioned DFC-sEV could be effectively used as an auxiliary method for periodontitis treatment via antioxidant effects in a subgingival environment, and loading it with HA is feasible and effective for clinical applications.

Keywords: small extracellular vesicle, dental follicle stem cell, periodontitis, reactive oxygen species, antioxidant effect

Introduction

Periodontal disease is the leading cause of adult tooth loss and a worldwide oral infectious disease.[1] Periodontitis is closely related to some systemic diseases, such as diabetes,[2] cardiovascular diseases,[3] Alzheimer's disease,[4] etc. Until now, clinical therapies have arrested the development of inflammation and achieved partial tissue repair, but the functional periodontal structure has been hard to rebuild.

Received: 24 November 2021
Accepted: 29 January 2022
Published: 22 February 2022

Dental follicle stem cells (DFSCs) have multiple superiorities, including easy accessibility, abundant sources, and active self-renewal ability.[5] Furthermore, DFSCs are beneficial for maintaining a favorable microenvironment and show a strong immunomodulatory ability.[6] However, stem cell therapy has some concerns in clinical practice, such as immune rejection of allogeneic cell implantation and survival and viability of stem cells.[7] Indeed, transplanted cells rapidly undergo apoptosis, necrosis, or other death mechanisms resulting from physical and active biochemical factors.[8] Therefore, it is necessary to find a suitable cell-free therapy.

The periodontium is a highly dynamic microenvironment that constantly undergoes turnover; under normal conditions, tissue formation is in balance with tissue degradation.[9] During periodontitis, inflammatory cytokines are upregulated and activate tissue degradation.[10,11] Even after nonsurgical therapies, inflammatory cytokines in gingival crevicular fluid from periodontitis patients are still unable to reach a healthy level.[12] Thus, the evaluation of the therapeutic effect of MSCs or derivatives should be carried out in an inflammatory environment. Recent studies have shown that disease-related preconditioned MSCs or MSCs-derived extracellular vesicles could exert powerful immunomodulatory effects on tissue repair,[13–15] such as interleukin and lipopolysaccharide (LPS). LPS, one of the most common virulence factors of the critical periodontal pathogen *P. gingivalis*, is enriched in the gingiva and peripheral blood of periodontitis and associated with the severity of periodontium dysfunction.[16,17] In our previous study, it was reported that *P. gingivalis* LPS enhanced the paracrine activity and immunomodulatory effect of DFSCs.[18]

Small extracellular vesicles (sEV) or exosomes can transfer biological molecules such as proteins, DNA, and miRNAs to exert biological effects and repair damaged tissues.[19,20] Exosomes play a role in cell communication and have been in the spotlight for their clinical applications in various diseases via changed microenvironments.[21] Exosomes have garnered much attention in the past decade due to their abundance in various biological fluids and ability to affect multiple organ systems.[22] It has been reported that the microenvironment related to disease alters the biological function of exosomes, which further argues that these vesicles can communicate important regulatory signals from one cell to another.[23]

Previous research found that LPS-preconditioned DFSCs -derived sEV is beneficial for repairing lost alveolar bone in rats,[18] while further study should be conducted on human-mimicking periodontitis models, and the main components, active ingredients and underlying mechanisms remain unclear. Therefore, we first performed a proteomic analysis of the components of dental follicle stem cells derived small extracellular vesicles (DFC-sEV) before and after LPS pretreatment to screen out essential proteins as a breakthrough to reveal their underlying mechanisms. In addition, the material properties, biological activity, and safety of the injectable loading system of sEV were determined and applied in the canine periodontitis model for preclinical application.

Materials and Methods

Animals

Animals were obtained from Dashuo Experimental Animal Co. Ltd. (Chengdu, China). This study was reviewed and approved by the Ethics Committees of the State Key Laboratory of Oral Diseases, West China School of Stomatology, Sichuan University. The approval number is WCHSIRB-D-2021-470. The care and use of the laboratory animals followed the guidelines of the Institutional Animal Care and Use Committee of West China School of Stomatology, Sichuan University.

Cell Culture

Human dental follicle stem cells (DFSCs) were obtained from mandibular embedded wisdom teeth, and periodontal ligament stem cells (PDLSCs) were isolated from premolars extracted for orthodontic treatment. All experiments were conducted by the ethical protocol approved by the Committee of Ethics of Sichuan University, and written informed consent was obtained from all guardians on behalf of the children and teenagers enrolled in this study. The approval number is WCHSIRB-D-2021-450. Primary cell culture protocols have been described in detail.[24]

Cells Characterization

Human DFSCs and PDLSCs were cultured in osteogenic medium or adipogenic medium, according to a previous study.[25] In addition, cells were incubated with FITC-conjugated antibodies against CD31, CD34, and CD90 and PE-conjugated antibodies against CD73 to determine the expression of cell surface markers. All antibodies were purchased from BD Biosciences. Flow cytometry was performed using the Beckman Coulter Cytomics FC500 MPL system (Beckman Coulter, Germany).

Preparation of sEV Isolation

The isolation of the sEV protocol has been described in detail.[18] Total exosome isolation reagent (Life, USA) was added to the concentrated solution, put into a 4 °C refrigerator overnight and centrifuged at 10,000 g for 1 h, and the sEV precipitate was stored in a −80 °C refrigerator for later use. Two types of sEV were characterized by transmission electron microscopy (TEM), nanoparticle tracking analysis (NTA), and Western blot. Each batch of sEV preparations was ascertained to have a similar size and markers (CD63, Hsp70, and Tsg101). The protein concentrations of sEV were assessed by a BCA assay kit (KeyGEN Biotech, Nanjing, China) following the manufacturers' instructions.

Proteomics Analysis of D-sEV and L-D-sEV

To analyze the proteomic composition of dental follicle stem cells -derived small extracellular vesicles (D-sEV) and LPS-preconditioned dental follicle stem cells-derived small extracellular vesicles (L-D-sEV), protein extracts of D-sEV and L-D-sEV were obtained with 3 repeats in each group. Protein concentration was determined via the BCA protein assay kit (Bio–Rad, USA). MS data were acquired using a data-dependent top 10 method dynamically choosing the most abundant precursor ions from the survey scan (300–1800 m/z) for HCD fragmentation. The MS raw data for each sample were combined and searched using MaxQuant 1.5.3.17 software for identification and quantitation analysis. The screening of the differentially expressed proteins (DEPs) was performed using MapDIA software by setting the fold change > 1.2 or < 0.83 and p value (P) < 0.05. We completed the bioinformatic analysis of DEPs, including subcellular localization (http://cello.life.nctu.edu.tw/), domain annotation, Gene Ontology (GO) annotation, Kyoto Encyclopedia of Genes and Genomes (KEGG) annotation (http://geneontology.org/), and protein–protein interaction (PPI) analysis (http://www.ebi.ac.uk/intact/).

Cell Proliferation and Migration Assay

Cell proliferation was measured using the cell counting kit-8 (CCK-8) assay (Beyotime, Shanghai, China). Cells were inoculated into 96-well plates at a concentration of 5×10^3 cells/well. Then, the cells were maintained in medium containing D-sEV or L-D-sEV. The optical density (OD) value was detected using a Multiskan Go spectrophotometer (Thermo Fisher Scientific).

Cell migration was determined by using Transwell chambers (8 mm pore, Corning, USA). PDLSCs were added to the upper chambers, while 500 μL medium was added to the bottom wells. After 24 h, cells that migrated to the submembrane surface were fixed with 4% paraformaldehyde for 20 min. Then, the membranes were stained with Giemsa staining solution (Solarbio, Beijing, China). After taking pictures under an optical microscope, the cells were manually counted, and the percentage of migrated cells to the number of inoculated cells was calculated.

Macrophage Culture and Treatment

RAW264.7 cells were obtained from the State Key Laboratory of Oral Diseases, West China School of Stomatology, Sichuan University, and cultured in RPMI (HyClone, USA) supplemented with 10% FBS at 37°C with 5% CO_2. To observe the uptake of sEV, macrophages were cocultured with DiO-labeled L-D-sEV or D-sEV in confocal dishes for 6 h, washed with PBS three times, and captured by confocal microscopy after staining with phallotoxins (Life Technologies, USA) and DAPI (Life Technologies, USA). To observe the effect of sEV on macrophage immunomodulation, macrophages were pretreated with sEV before the addition of murine IL-4 (50 ng/mL, 4 h). The CD206 and Arg-1 gene levels were measured, and CD206 and F4/80 double-positive percentages were measured by flow cytometry (Beckman

Coulter). To further explore the underlying mechanism, macrophages were treated with sEV, and cells were harvested to measure target genes and proteins.

ROS Level Assay

According to the manufacturer's instructions, reactive oxygen species (ROS) levels were determined using an ROS Assay Kit (Beyotime, Shanghai, China). DCFH-DA diluent was added to the cells followed by 30 min incubation at 37°C, and the cells were analyzed by flow cytometry.

Preparation and Characterization of HA/sEV

sEV was dissolved in PBS, mixed with Gengigel® (RICERFARMA SRL, Italy) containing 0.2% hyaluronic acid gel (HA) in different volume ratios (0.5, 0.25, 0.125), and stored at 4 °C for later application. In this study, HA was used to refer to 0.2% hyaluronic acid gel. At 25±2°C, the samples were further tested for viscoelastic and rheological properties using a rheometer (HAAKE Viscotester iQ, Germany). An aliquot of 400 μL of sEV-loaded HA (HA/sEV) was loaded into the rheometer. The value of G' and G" of each sample was recorded.

To assess the release profile, the sEV-loaded HA was incubated in 200 μL PBS at 37 °C in an incubator temperature, supernatant samples were collected on days 1, 2, 3, 5, and 7, and then the concentration of protein in the supernatant was measured by the BCA protein assay kit (KeyGEN Biotech, Nanjing, China).

In vitro Bioactivity of HA/sEV

PDLSCs were seeded in 96-well plates at a density of 3×10^3 cells/well and cultured overnight at 37°C. To select the appropriate percentage of HA in the medium that had no significant effect on cell proliferation, the cells were cocultured with medium containing 5%, 10%, or 20% HA. To explore the impacts of sEV-loaded HA on cell viability, cells were cocultured with 5% sEV-loaded HA containing 200 μg/mL sEV. Cell viability was measured by CCK-8 assay (Beyotime, Shanghai, China).

In situ Evaluation of HA/sEV in vivo

Four 1-year-old healthy beagle dogs (10 kg, male) were used in this experiment. All surgical procedures were performed under general and local anesthesia according to a previous study.[26] Briefly, two walls of intrabony defects (2 mm (mesiodistal width) ×3 mm (depth)×6 mm (height from the cement-enamel junction)) were surgically created on the mesial side of mandibular third and fourth premolars bilaterally. The cementum was removed by Gracey curettes, and the notch was made in the root extension of the defect. Subsequently, a bacterial plaque retentive silk ligature (3–0) was placed in the gingival sulcus for 1 month to induce experimental periodontitis. After the thread silk was removed, dental plaque and calculus were removed by supragingival and subgingival debridement with hand instruments. Dogs in the periodontitis (PD) group were treated with dental plaque control. In the PBS group, a 50 μL PBS-loaded HA system was administered using a 1 mL syringe. In the D-sEV or L-D-sEV group, a 50 μL sEV-loaded HA system (including 200 μg sEV) was injected into the periodontal pocket. The administration frequency was once a week for four consecutive administrations. After 8 weeks of administration, mandible specimens were collected. Blood samples from a vein of the lower limb of dogs were obtained at different time points.

Micro-CT Tomography Evaluation

All samples were measured using micro-CT as previously described.[26] A SkyScan 1176 desktop X-ray micro-CT system (Skyscan, Belgium) was used to scan all the specimens. These data were reconstructed by NRecon (Skyscan, Belgium) cone-beam reconstruction software and were analyzed by DataViewer. For bone morphometric analysis, bone volume/total volume (BV/TV) and trabecular separation (Tb. Sp) were measured.

Histology and Immunohistochemistry Analysis

All bone specimens were decalcified, dehydrated in an ascending series of ethanol solutions, and embedded in paraffin. Serial sections (5 μm) were obtained and stained with hematoxylin-eosin (H&E) staining, Masson staining, and

immunofluorescence analysis according to the manufacturer's recommended protocol. The width of the new periodontal ligament (PDL) was the average width at the point of the apical notch, alveolar crest and middle of the apical notch to the alveolar crest. The number of vessels was defined as the total number of vessels per square millimeter. The average fluorescence density was measured using ImageJ software. Each assay was run in triplicate.

qRT–PCR

Total RNA was isolated using TRIzol reagent according to the manufacturer's protocol (TIANMO BIOTECH, Beijing, China). RNA (1 μg) was converted into cDNA with an iScript cDNA synthesis kit (Vazyme, Nanjing, China). Gene expression was quantified by the 2−ΔΔCt method using GAPDH expression as an internal control. The target gene primers used are listed in Supplementary Table 1.

Western Blot

Cells were lysed in RIPA buffer (KeyGEN Biotech, Nanjing, China) with 1 mM proteinase inhibitor phenylmethanesulfonyl fluoride added for 30 min, and then the protein was extracted. The membranes were blotted with antibodies, which are listed in Supplementary Table 2. The relative intensity of the tested protein was quantitatively analyzed by the ratio of the gray value between the target protein and GAPDH in the same sample.

Statistical Analysis

All data are expressed as the mean ± standard error of the mean (SEM) for three independent experiments and analyzed using GraphPad Prism 8.0.2. Comparisons between two groups were performed using nonparametric unpaired two-tailed Student's *t* test. $P < 0.05$ was considered statistically significant.

Results

Identification of Cells and sEV

DFSCs and PDLSCs were successfully extracted from dental follicles and PDL, respectively (Figure 1A a and B a). After being cultured in conditioned medium for 2 weeks, the calcified nodes and lipid droplets were positively stained in both cell lines (Figure 1A b-c and B b-c). The extracted cells were identified by flow cytometry (Figure 1C and D). These results showed that the extracted cells were DFSCs and PDLSCs.

D-sEV and L-D-sEV were isolated by polyethylene glycol (PEG), which can extract sEV whose distribution and morphology are similar to those of ultracentrifugation, with faster and more convenient procedures. Low concentrations of LPS (150, 200, and 250 ng/mL) significantly promoted DFSCs proliferation, and 250 ng/mL LPS was chosen as the stimulatory factor due to its most potent ability to promote cell proliferation (Supplementary Figure 1A). Secretion and morphological characterization of D-sEV and L-D-sEV were further analyzed: morphological characterization of D-sEV and L-D-sEV were the same, while L-D-sEV was extracted more after treated by LPS compared with that of D-sEV at the same number of DFSCs (26.94 ± 2.717 μg/10^5 cells vs 18.16 ± 0.7784 μg/10^5 cells) (Supplementary Figure 1B). D-sEV and L-D-sEV exhibited double-membrane shapes (Figure 1E) and were approximately 120 nm in size (Figure 1F). Both D-sEV and L-D-sEV expressed CD63, Tsg101, and Hsp70 (Figure 1G).

Quantitative Proteomic Analysis of D-sEV and L-D-sEV

We analyzed the DEPs between the two groups defined as 1.2-fold for upregulated and 0.83-fold for downregulated proteins ($P < 0.05$), and thirty-eight DEPs were identified in L-D-sEV vs D-sEV. These DEPs included 11 upregulated proteins (Table 1), 12 downregulated proteins (Table 2), and 15 proteins only detected in D-sEV or L-D-sEV (Table 3).

The GO categories of the DEPs were ascertained to characterize them according to biological processes, cellular components, and molecular functions (Figure 2A). The results indicated that the identified DEPs were involved in biological processes associated with cellular processes, biological regulation, regulation of biological process, metabolic processes, response to stimuli, cellular component organization of biogenesis, positive regulation of biological process, multicellular organism process, signaling, localization, etc. (Figure 2A). The molecular functions

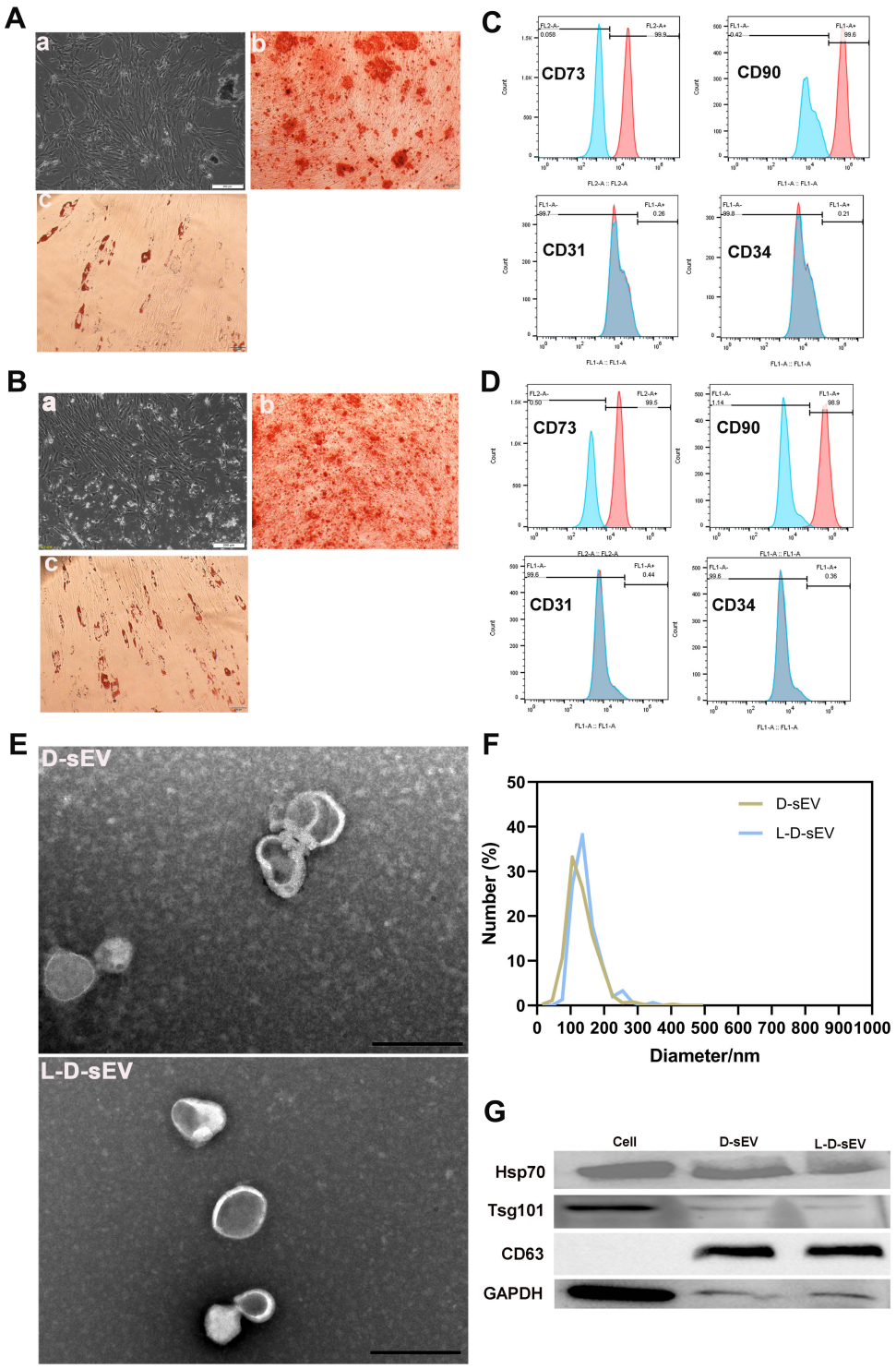

Figure 1 Identification of cells and sEV. (**A** a and **B** a) DFSCs and PDLSCs morphology under an optical microscope. Scale bar: 200 μm. (**A** b and **B** b) Representative pictures after osteogenesis induction for 2 weeks. Scale bar:100 μm. (**A** c and **B** c) Representative pictures after adipogenesis induction for 2 weeks. Scale bar:100μm. (**C**) Flow cytometry detection of the cell markers CD90, CD73, CD31, and CD34 in DFSCs. (**D**) Flow cytometry detection of the cell markers CD90, CD73, CD31, and CD34 in PDLSCs. (**E**) TEM analysis was performed and verified that D-sEV and L-D-sEV were double-membrane shapes with diameters between 30 and 150 nm. Scale bar: 200 nm. (**F**) Size distribution of D-sEV and L-D-sEV as determined by NTA. (**G**) Western blot for Hsp70, Tsg101, CD63, and GAPDH in DFSCs, D-sEV, and L-D-sEV.

of the identified DEPs were specifically associated with binding, catalytic activity, structural molecule activity, molecular function regulator, molecular transducer activity, antioxidant activity and transcription regulator activity, which were essential in L-D-sEV.

Table 1 List of the Up-Regulated Proteins in L-D-sEV vs D-sEV

Protein Name	Gene Name	Molecular Function	Cellular Component	L-D-sEV/ D-sEV	t test p value
Glutathione reductase	GSR	Antioxidant activity; oxidoreductase activity; catalytic activity; binding	Mitochondrial	1.9767	0.0146
Protein disulfide-isomerase A6	PDIA6	Catalytic activity; oxidoreductase activity	Endoplasmic reticulum	1.7533	0.0318
Protein S100-A1	S100A1	Binding	Cytoplasmic	1.690	0.027
Peptidyl-prolyl cis-trans isomerase A	PPIA	Catalytic activity; binding	Cytoplasmic	1.5994	0.0234
Angiopoietin-related protein 3	ANGPTL3	Binding; molecular function regulator	Nuclear	1.5170	0.0183
Syndecan-4	SDC4	Binding; molecular transducer activity	Cytoplasmic; Nuclear	1.5144	0.0498
Actin-related protein 2/3 complex subunit 4	ARPC4	Structural molecule activity; binding	Cytoplasmic; Mitochondrial	1.4568	0.0370
Follistatin	FST	Binding; molecular function regulator	Extracellular	1.3701	0.0092
Decorin	DCN	Structural molecule activity; binding	Extracellular; Nuclear	1.3246	0.0026
Thrombospondin-2	THBS2	Binding	Extracellular	1.2355	0.02102
NADP-dependent malic enzyme	ME1	Catalytic activity; binding; oxidoreductase activity	Cytoplasmic	1.2247	0.0367

These proteins were divided into two general categories: molecular functions category and binding proteins category (Tables 1-3). The following proteins were involved in catalytic activity: Glutathione reductase (GSR), Protein disulfide-isomerase A6 (PDIA6), Peptidyl-prolyl cis-trans isomerase A (PPIA), NADP-dependent malic enzyme (ME1), L-xylulose reductase (DCXR), Ubiquitin carboxyl-terminal hydrolase isozyme L1 (UCHL1), Fumarate hydratase (FH), Lysosomal protective protein (CTSA), Inactive tyrosine-protein kinase 7 (PTK7), Lactotransferrin (LTF), Dual specificity mitogen-activated protein kinase kinase 1 (MAP2K1), Prolyl 4-hydroxylase subunit alpha-2 (P4HA2), Superoxide dismutase [Cu-Zn] (SOD1), Hepatocyte growth factor receptor (MET), Creatine kinase B-type (CKB), 40S ribosomal protein S3 (RPS3), Palmitoyl-protein thioesterase 1(PPT1), Ephrin type-A receptor 4 (EPHA4), Prostaglandin E synthase 3 (PTGES3), Protein phosphatase 1A (PPM1A) and Eukaryotic translation initiation factor 2 subunit 3B (EIF2S3B). GSR, PDIA6, ME1, DCXR, P4HA2 and SOD1 were involved in antioxidant and oxidoreductase activity. The interaction network of the DEPs revealed that GSR, ME1, PDIA6, FH, and SOD1 showed interactions, as shown in Figure 2B.

The KEGG pathway analysis showed that the identified DEPs were enriched in the PI3-AKT signaling pathway, focal adhesion, ECM-receptor metabolism, mitogen-activated protein kinase (MAPK) signaling pathway, Fc gamma R-mediated phagocytosis, and regulation of actin cytoskeleton (Figure 2C).

L-D-sEV Inhibited the RANKL/OPG Ratio in PDLSCs by Inhibiting ROS/JNK Signaling

D-sEV or L-D-sEV promoted the proliferation and migration of PDLSCs in vitro (Figure 3A and B). ROS, known as a trigger or mediator of MAPK family members, have a substantial effect on multiple usual biochemical roles and pathological progressions.[27] We found that ROS levels were significantly reduced in PDLSCs after D-sEV or L-D-sEV treatment for 4 h under inflammatory conditions, and ROS levels in the L-D-sEV group were lower than those in the D-sEV group ($P<0.01$). After 8 h, the ROS levels were not significantly reduced in the D-sEV group compared with the

Table 2 List of the Down-Regulated Proteins in L-D-sEV vs D-sEV

Protein Name	Gene Name	Molecular Function	Cellular Component	L-D-sEV/ D-sEV	t test p value
Neurogenic locus notch homolog protein 1	NOTCH1	Transcription regulator activity; binding; molecular function regulator; molecular transducer activity	Extracellular	0.8134	0.0170
L-xylulose reductase	DCXR	Catalytic activity; binding; oxidoreductase activity	Mitochondrial	0.7964	0.0094
Plexin domain-containing protein 2	PLXDC2	Not retrieved	PlasmaMembrane; Nuclear	0.7497	0.0320
Ubiquitin carboxyl-terminal hydrolase isozyme L1	UCHL1	Catalytic activity; binding	Cytoplasmic	0.7369	0.0482
Laminin subunit alpha-1	LAMA1	Structural molecule activity; binding	Extracellular	0.7293	0.0298
Fumarate hydratase, mitochondrial	FH	Catalytic activity; binding	Mitochondrial	0.7174	0.0350
Lysosomal protective protein	CTSA	Catalytic activity; molecular function regulator	Lysosomal	0.7033	0.0350
Collagen alpha-1(XIV) chain	COL14A1	Structural molecule activity; binding	Cytoplasmic; Nuclear	0.6954	0.0239
Inactive tyrosine-protein kinase 7	PTK7	Catalytic activity; binding; molecular transducer activity	Cytoplasmic; Nuclear	0.6896	0.0137
Lactotransferrin	LTF	Catalytic activity; binding; molecular function regulator	Extracellular	0.6133	0.0307
Dual specificity mitogen-activated protein kinase kinase 1	MAP2K1	Catalytic activity; structural molecule activity; binding; molecular function regulator	Cytoplasmic; Nuclear	0.5590	0.0412
Protein sidekick-1	SDK1	Binding	PlasmaMembrane; Nuclear	0.5110	0.0497

LPS group (Figure 3C), while the ROS levels were significantly decreased in the L-D-sEV group compared with the D-sEV group or LPS group (Figure 3D). An increased ratio of NF-kB receptor activator (RANKL) and osteogenic protective protein (OPG) indicates bone resorption.[28] Under normal conditions, D-sEV and L-D-sEV did not change the RANKL/OPG ratio compared with the Con group (Figure 3E and F). Under inflammatory conditions, L-D-sEV and D-sEV inhibited the RANKL/OPG ratio compared with that of the LPS group, and a more robust decrease in the RANKL/OPG ratio was observed in the L-D-sEV group ($P<0.05$) (Figure 3G and H). Meanwhile, MAPK pathways including extracellular signal-related kinases (ERK) and Jun amino-terminal kinases (JNK) signaling have been proven to be essential in osteoclast differentiation and activation.[29] L-D-sEV or D-sEV treatment significantly decreased the p-JNK/JNK ratio under normal ($P<0.01$) and inflammatory conditions ($P<0.001$). However, the ERK pathway was not affected (Figure 3E-H). A JNK inhibitor (SP600125) significantly reduced the RANKL/OPG ratio ($P<0.001$), which was consistent with L-D-sEV in inflammatory PDLSCs (Figure 3I). These results showed that DFC-sEV tended to regulate the bone homeostasis of inflammatory PDLSCs but did not affect healthy PDLSCs. DFC-sEV exerted antioxidant activity by inhibiting ROS/JNK signaling (Figure 3J).

L-D-sEV Induced Macrophage Polarization by Inhibiting Oxidative Stress

In response to microenvironmental stimuli, macrophages can be activated and polarize to proinflammatory M1 and/or anti-inflammatory M2.[30,31] M2 macrophages contribute to bone tissue repair and inflammation reduction.[32] First, D-sEV

Table 3 List of the Detected or Undetected Proteins in L-D-sEV vs D-sEV

Protein Name	Gene Name	Molecular Function	Cellular Component	L-D-sEV	D-sEV
Actin-related protein 2/3 complex subunit 1B	ARPC1B	Structural molecule activity; binding;	Extracellular	Detected	Undetected
Prolyl 4-hydroxylase subunit alpha-2	P4HA2	Catalytic activity; binding; oxidoreductase activity	Endoplasmic reticulum	Detected	Undetected
Superoxide dismutase [Cu-Zn]	SOD1	Antioxidant activity; catalytic activity; binding; oxidoreductase activity	Cytoplasmic	Detected	Undetected
Hepatocyte growth factor receptor	MET	Catalytic activity; binding; molecular transducer activity	PlasmaMembrane	Detected	Undetected
Creatine kinase B-type	CKB	Catalytic activity; binding	Cytoplasmic	Detected	Undetected
Ribonuclease inhibitor	RNH1	Molecular function regulator	Cytoplasmic	Detected	Undetected
Tenascin-X	TNXB	Structural molecule activity; binding	Nuclear	Detected	Undetected
Heterogeneous nuclear ribonucleoproteins A2/B1	HNRNPA2B1	Binding	Nuclear	Detected	Undetected
40S ribosomal protein S3	RPS3	Catalytic activity; structural molecule activity; binding	Cytoplasmic	Detected	Undetected
Palmitoyl-protein thioesterase 1	PPT1	Catalytic activity; binding	Lysosomal	Detected	Undetected
Ephrin type-A receptor 4	EPHA4	Catalytic activity; binding; molecular transducer activity	PlasmaMembrane; Cytoplasmic	Detected	Undetected
Prostaglandin E synthase 3	PTGES3	Catalytic activity; binding	Nuclear	Detected	Undetected
Neuronal pentraxin-1	NPTX1	Binding	Extracellular; Cytoplasmic; Mitochondrial	Detected	Undetected
Protein phosphatase 1A	PPM1A	Catalytic activity; binding	Cytoplasmic	Undetected	Detected
Eukaryotic translation initiation factor 2 subunit 3B	EIF2S3B	Catalytic activity; binding	Cytoplasmic; Mitochondrial	Undetected	Detected

and L-D-sEV could be taken up by RAW264.7 cells and promoted the proliferation of macrophages in a dose-dependent manner (Figure 4A and B). sEV treatment significantly increased the gene expression of the M2 surface markers Arg-1 and CD206, especially at a dose of 50 μg/mL (Figure 4C). The CD206(+) F4/80(+) percentage was increased after 50 μg/mL D-sEV or L-D-sEV treatment (Figure 4D). These results showed that D-sEV and L-D-sEV could promote M2 polarization in a proper dose range.

Previous studies found that oxidative stress (OS) or ROS production was involved in macrophage differentiation, and an increase in the ratio of the reduction of oxidized glutathione (GSSG) to reduced glutathione (GSH) indicates OS.[33,34] Both D-sEV and L-D-sEV exhibited the anti-OS response, and L-D-sEV was more effective in antioxidation and promotion of M2 polarization due to the significant decrease in ROS levels (Figure 5A). In addition, the ratio of GSSG to GSH in the D-sEV and L-D-sEV groups was significantly lower than that in the Con group and was the lowest in the L-D-sEV-treated group (Figure 5B). L-D-sEV, which contained more GSR, had a more potent antioxidant effect through endocytosis to lower the ratio of GSSG/GSH.

MAPK/ERK signal is proved to be related to OS.[34] Both D-sEV ($P<0.01$) and L-D-sEV ($P<0.05$) treatment upregulated the p-ERK/ERK ratio. After applying ERK inhibitor (u1206), the p-ERK/ERK was reduced, and D-sEV

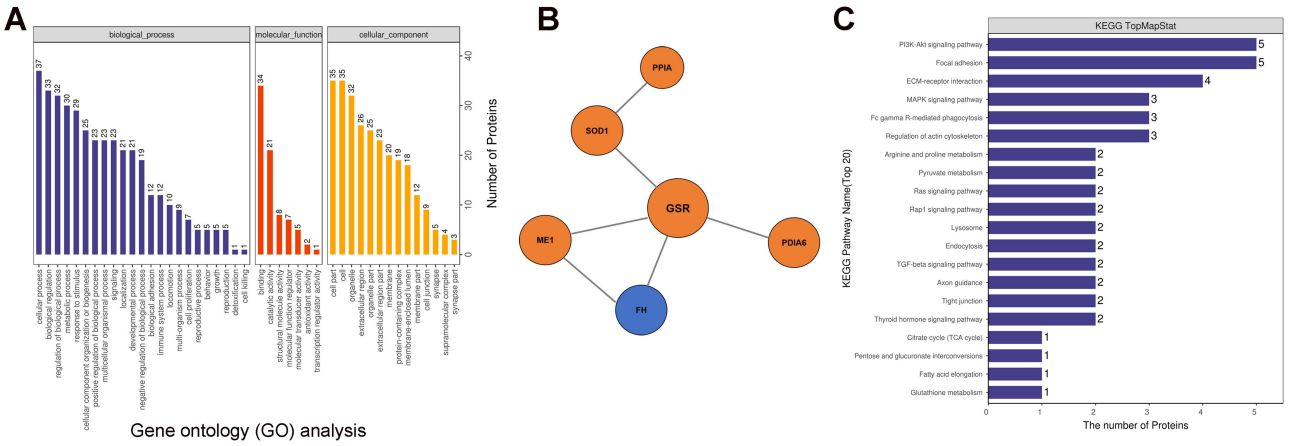

Figure 2 Quantitative proteomic analysis of D-sEV and L-D-sEV. (**A**) Gene ontology (GO) analysis of the DEPs in L-D-sEV vs D-sEV. The right coordinate axis indicates the number of proteins for each GO annotation, and the lower coordinate axis indicates the GO annotations. Blue stripes indicate biological process categories of DEPs; red stripes indicate categories of molecular functions; yellow stripes indicate categories of cellular components. (**B**) PPI analysis of some DEPs related to antioxidant activity. (**C**) KEGG annotation analysis of DEPs in L-D-sEV vs D-sEV.

(P<0.05) or L-D-sEV (P<0.05) treatment could reactive the ERK signaling (with p-ERK/ERK ratio elevation) (Figure 5C and D). In addition, to explore the effects of ERK signaling on antioxidants, we measured SOD1 and SOD2 expression, which is essential in defending tissues against OS and inhibiting ROS elevation.[35] SOD1 was significantly increased in the D-sEV and L-D-sEV groups, and SOD1 expression was the highest in the L-D-sEV group. SOD2 expression was not upregulated considerably after treatment with D-sEV or L-D-sEV (Figure 5C and D). D-sEV and L-D-sEV significantly reduced ROS levels in macrophages. After the application of u1206, ROS levels were significantly upregulated (P<0.01), and D-sEV and L-D-sEV significantly inhibited ROS levels again (P<0.01) (Figure 5E). These data demonstrated that sEV could exert antioxidant effects through multiple signaling pathways, including the ERK pathway (Figure 5F).

Characteristic of HA/sEV System in vitro

The production process of the sEV injectable system is shown in Figure 6A. With the increase in PBS with sEV, the material viscosity decreases, and the fluidity increases (Figure 6B and C). The best proper volume ratio of PBS and HA owing to matchable viscosity and fluidity was 0.125. The release rate of D-sEV by HA was the fastest at 24 h, which was approximately 48.01% of the total D-sEV, and after 7 days, it reached 83.3%. The percentage of L-D-sEV released by HA was approximately 46% in 24 h, and the percentage reached 71.71% after 7 days (Figure 6D and E). Only 5% HA can promote cell proliferation, so 5% was chosen as the ideal concentration for carrying sEV. Moreover, compared with the HA group, the sEV released by HA significantly promoted the proliferation and migration of PDLSCs. Its effect on cell migration was not different from that of sEV alone (Figure 6F and G). These results demonstrated that HA was an appropriate carrier.

HA/sEV Promoted Periodontal Regeneration in vivo

After administration of HA/sEV in dogs for 8 weeks, new alveolar bone and PDL-like structures were regenerated, and L-D-sEV had the best effect. Micro-CT analysis indicated that BV/TV% was increased in the L-D-EV group compared with that of the other groups. In addition, the Tb. Sp in the PBS, D-sEV, and L-D-sEV groups were decreased compared with that of the PD group (Figure 7A and B). In these sEV groups, the arrangement of the periodontal ligament was regular, dense, and wider, and more Sharpey's fibers were attached perpendicularly to the cementum-like tissue layer (Figure 7C and D). The PDL width and number of vessels in the PDL were significantly increased in the L-D-sEV group compared with the PD group (P<0.05) (Figure 7E and F). Additionally, the PDL biomarker Periostin expression was significantly elevated in the D-sEV group (P<0.05) and L-D-sEV group (P<0.01) compared with that in the PD group

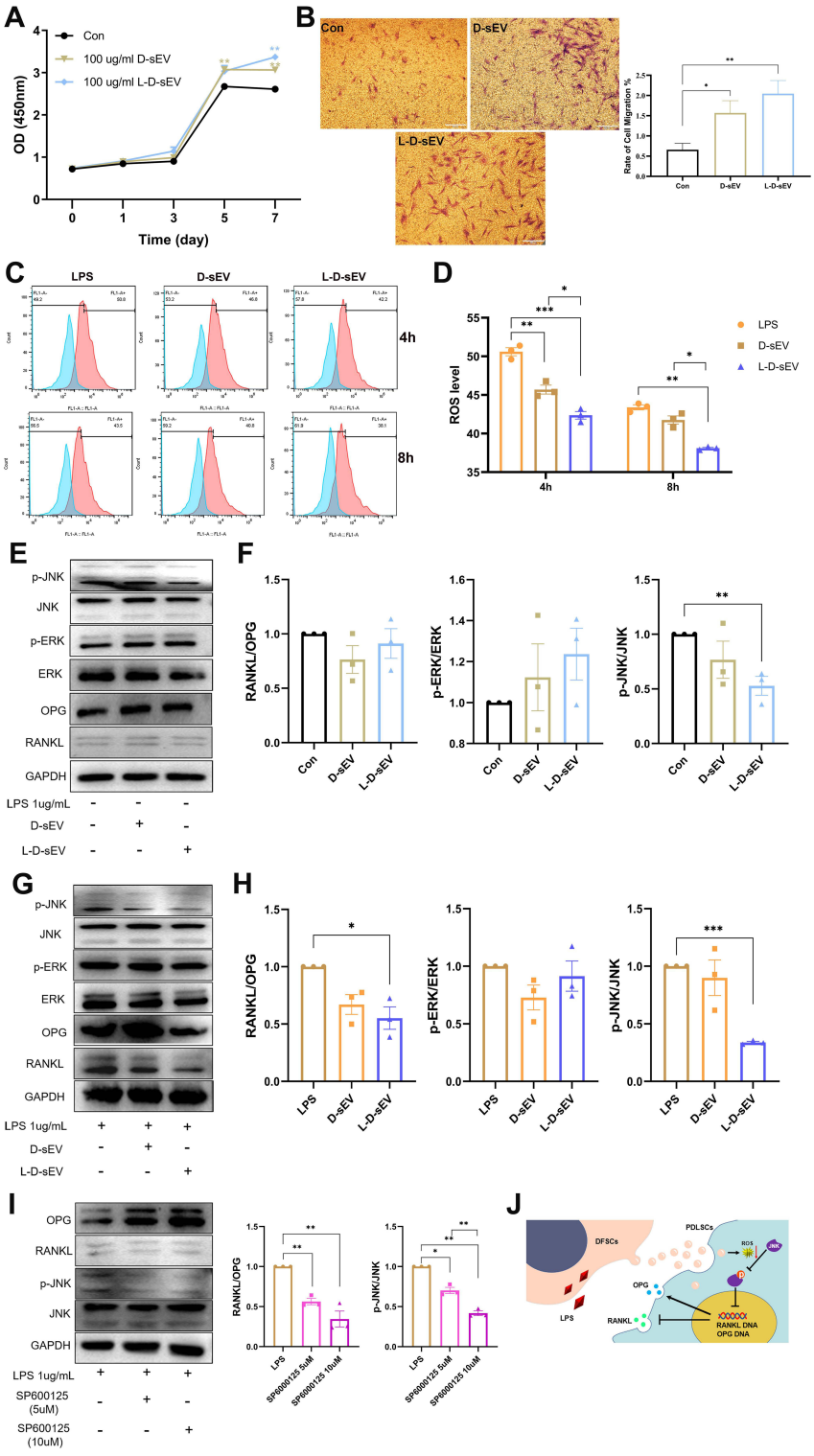

Figure 3 L-D-sEV inhibited the RANKL/OPG ratio in PDLSCs via ROS/JNK signaling under inflammatory conditions. (**A**) PDLSCs were cocultured with (100 μg/mL) D-sEV or L-D-sEV, and cell viability was measured by CCK-8 assay. (**B**) Representative images of the cell migration assay and quantitative analysis. Scale bar: 200 μm. (**C**) Intracellular ROS levels were measured by flow cytometry. PDLSCs were pretreated with LPS (1 μg/mL, 24 h) and then cocultured with D-sEV or L-D-sEV (100 μg/mL, 4 h or 8 h). (**D**) Quantitative analysis of intracellular ROS levels. (**E**) The JNK, p-JNK, ERK, p-ERK, OPG and RANKL protein levels were measured by Western blot. PDLSCs were cocultured with D-sEV or L-D-sEV (100 μg/mL, 48 h). (**F**) Quantitative analysis of the protein bands in Figure 3E. (**G**) The JNK, p-JNK, ERK, p-ERK, OPG and RANKL protein levels were measured by Western blot. PDLSCs were stimulated with LPS (1 μg/mL, 24 h) and then cocultured with D-sEV or L-D-sEV (100 μg/mL, 48 h). (**H**) Quantitative analysis of the protein bands in Figure 3G. (**I**) The OPG, RANKL, JNK, and p-JNK protein levels were measured by Western blot and quantitative analysis. PDLSCs were incubated with LPS (1 μg/mL, 24 h) and then stimulated with SP600125 (5 μM, 10 μM) for 24 h. (**J**) DFSC-sEV inhibited the RANKL/OPG ratio via ROS/JNK signaling. Data are shown as the mean ± SEM for three independent experiments. *P < 0.05; **P < 0.01; ***P < 0.001.

https://doi.org/10.2147/IJN.S350869 DovePress

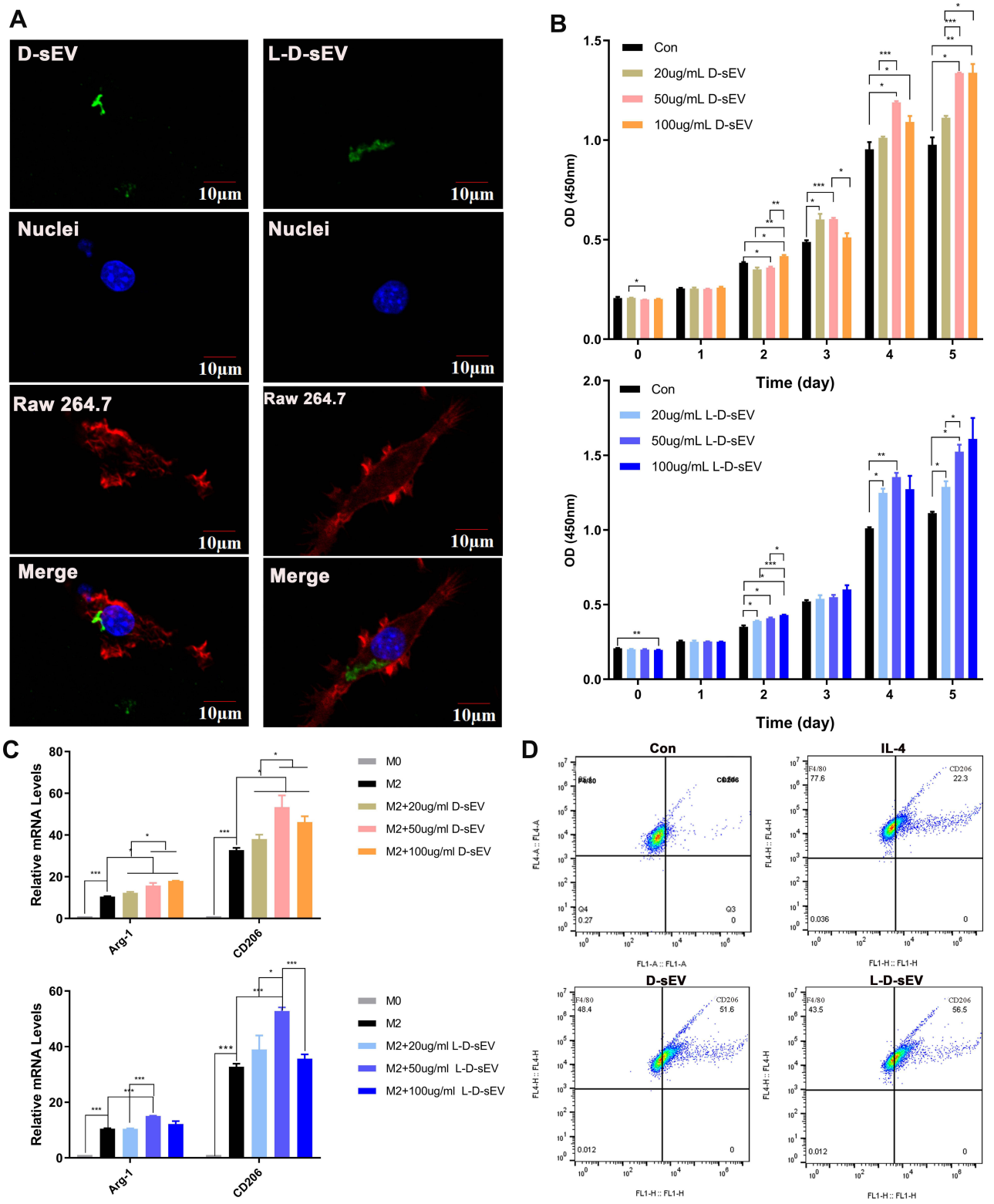

Figure 4 L-D-sEV promoted macrophage proliferation and M2 polarization. (**A**) Uptake analysis of D-sEV and L-D-sEV by RAW264.7 cells (red: phalloidin, green: DiO-labeled sEV, blue: DAPI-labeled nuclei). Scale bar: 10 μm. (**B**) RAW264.7 cells were cocultured with (20, 50, or 100 μg/mL) D-sEV or L-D-sEV, and cell viability was measured by CCK-8 assay. (**C**) The Arg-1 and CD206 gene levels of RAW264.7 cells were measured by qRT–PCR. (**D**) The percentage of M2 macrophages was measured by flow cytometry. Double-positive cells (CD206 and F4/80) represented M2 macrophages. Data are shown as the mean ± SEM for three independent experiments. *P < 0.05; **P < 0.01; ***P < 0.001.

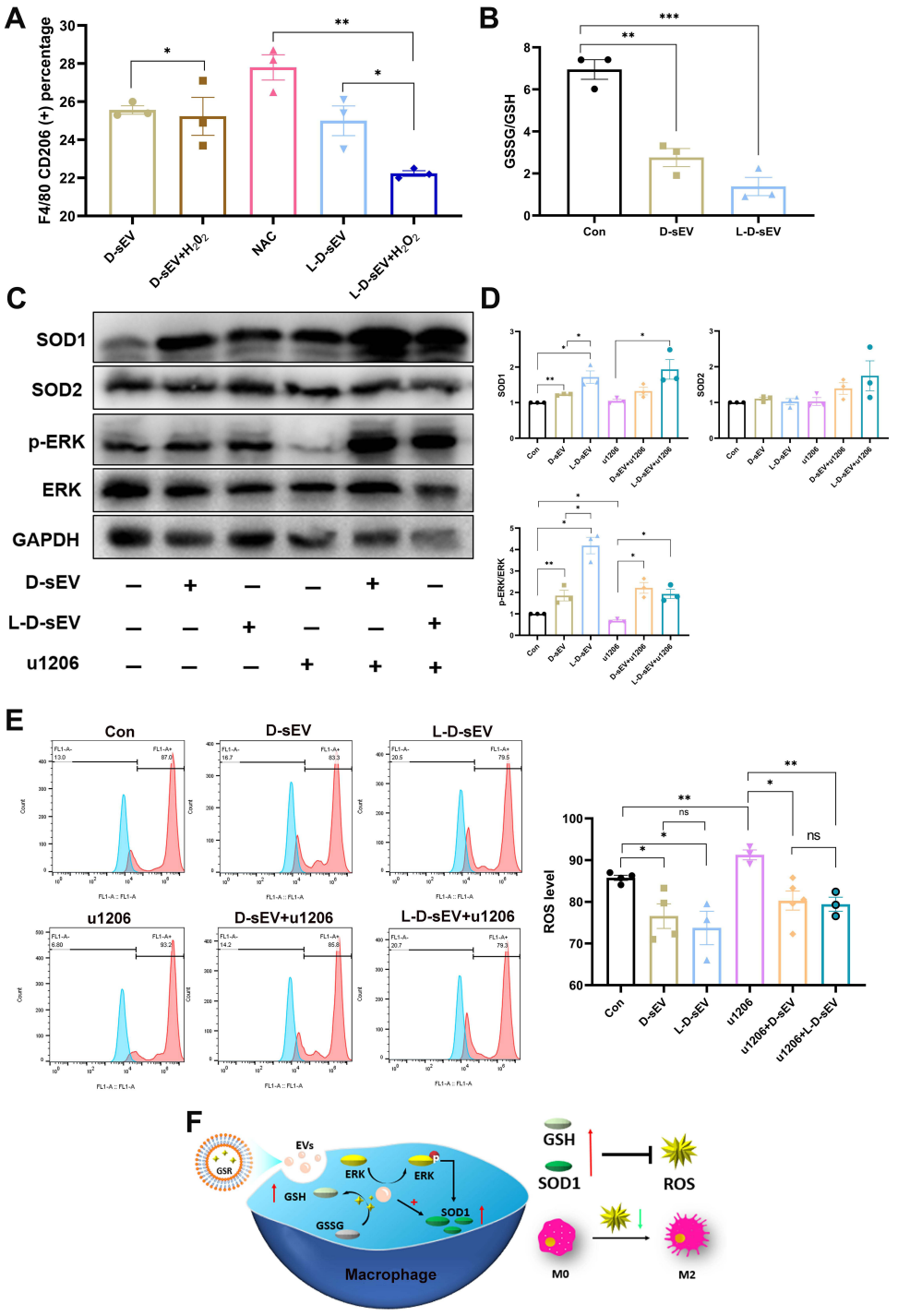

Figure 5 L-D-sEV promoted M2 polarization via ROS/ERK signaling. (**A**) The percentage of M2 macrophages was measured by flow cytometry. RAW264.7 cells were treated with D-sEV or L-D-sEV (50 μg/mL, 6 h) with or without 25 μM H_2O_2 or 10 mM NAC stimulation. (**B**) The GSSG/GSH ratio of macrophage. RAW264.7 cells were treated with D-sEV or L-D-sEV (50 μg/mL, 6 h). (**C**) The SOD1, SOD2, ERK and p-ERK protein levels were measured by Western blot. Raw264.7 Cells were first pretreated with or without u1206 (10 μM, 30 min) and then cocultured with or without D-sEV or L-D-sEV (50 μg/mL, 6 h). (**D**) Quantitative analysis of the protein bands in Figure 5C. (**E**) Intracellular ROS levels were measured by flow cytometry and quantitative analysis. RAW264.7 cells were first pretreated with or without u1206 (10 μM, 30 min) and then cocultured with or without D-sEV or L-D-sEV (50 μg/mL, 6 h). (**F**) Illustration showing that sEV promotes M2 polarization via SOD1/ERK-mediated ROS. Data are shown as the mean ± SEM for three independent experiments. *P < 0.05; **P < 0.01; ***P < 0.001.

(Figure 7G and H). The above results demonstrated that sEV promoted periodontal tissue regeneration and that L-D-sEV was more effective.

In the L-D-sEV group, CD206 expression in the new bone zone was significantly increased compared with that in the PD group or PBS group (P<0.01) (Figure 7I and J). In the D-sEV group, the RANK/OPG ratio was decreased compared

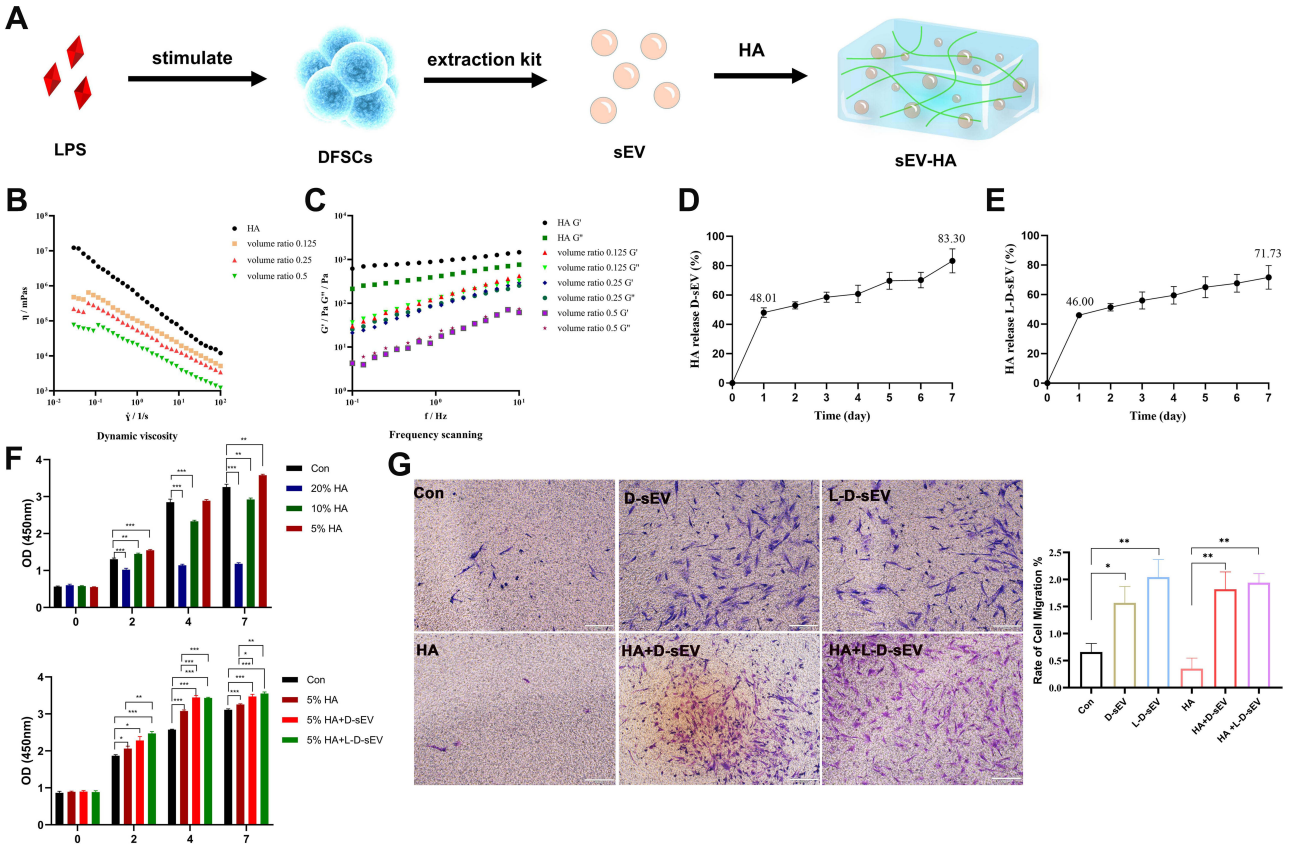

Figure 6 Physical and biological characterization of HA/sEV. (**A**) The schematic diagram of material construction. (**B**) The dynamic viscosity of the mixture of sEV (dissolved in PBS) and HA with different volume ratios (0.125, 0.25, 0.5). (**C**) The frequency scanning analysis. (**D**) Release experiment of the D-sEV-loaded HA. (**E**) Release experiment of the L-D-sEV-loaded HA. (**F**) The effect of (5%, 10%, 20%) HA or 5% HA with D-sEV or L-D-sEV (200 μg/mL) on PDLSCs viability was measured by CCK-8 assay. (**G**) Representative images of the cell migration assay and quantitative analysis. Scale bar: 200 μm. Data are shown as the mean ± SEM for three independent experiments. *P < 0.05; **P < 0.01; ***P < 0.001.

with that in the PD group or the PBS group (P<0.01). Similarly, compared with the PD group (P<0.001) or PBS group (P<0.01), the RANKL/OPG ratio was significantly reduced in the L-D-sEV group. Compared with that in the D-sEV group, RANKL/OPG expression was also inhibited in the L-D-sEV group (P<0.05) (Figure 7K-M). These results were consistent with data in vitro. Decreases in the RANKL/OPG ratio and elevation of M2 both benefited new bone formation. The serum complement (C3, C4), immunoglobulin (IgA, IgG, IgM), and CRP levels were measured to evaluate the safety of HA/sEV. As shown in Table 4, serum C3, C4, IgA, IgG, IgM, and CRP levels fluctuated slightly around average levels in the following month after surgery, IgG levels were significantly decreased after applying HA/sEV for 4 weeks and 8 weeks, compared with that of the periodontitis dogs. All data indicated that local implantation of xenogeneic sEV did not cause obvious immune rejection in dogs.

Discussion

Well-established proteomics information about the interaction between proteins and their biological relevancies was used to further clarify the effects of LPS on D-sEV protein contents and biological function. DEPs between D-sEV and L-D-sEV were divided into categories that highlighted the protein functions of cell binding and enzyme regulation or activity. The biological process analysis showed that most of these proteins are involved in the cellular process, biological regulation, regulation of biological processes, metabolic processes, and response to stimulus, indicating that the identified protein expression pattern may reflect the change in the L-D-sEV.

In this proteomics study, the identified DEPs were shown to be involved mainly in binding and catalytic activity (oxidation activity and oxidoreductase activity). When DFSCs are exposed to an inflammatory microenvironment, they can mount an adaptive response by releasing cytokines or small extracellular vesicles to the regulated

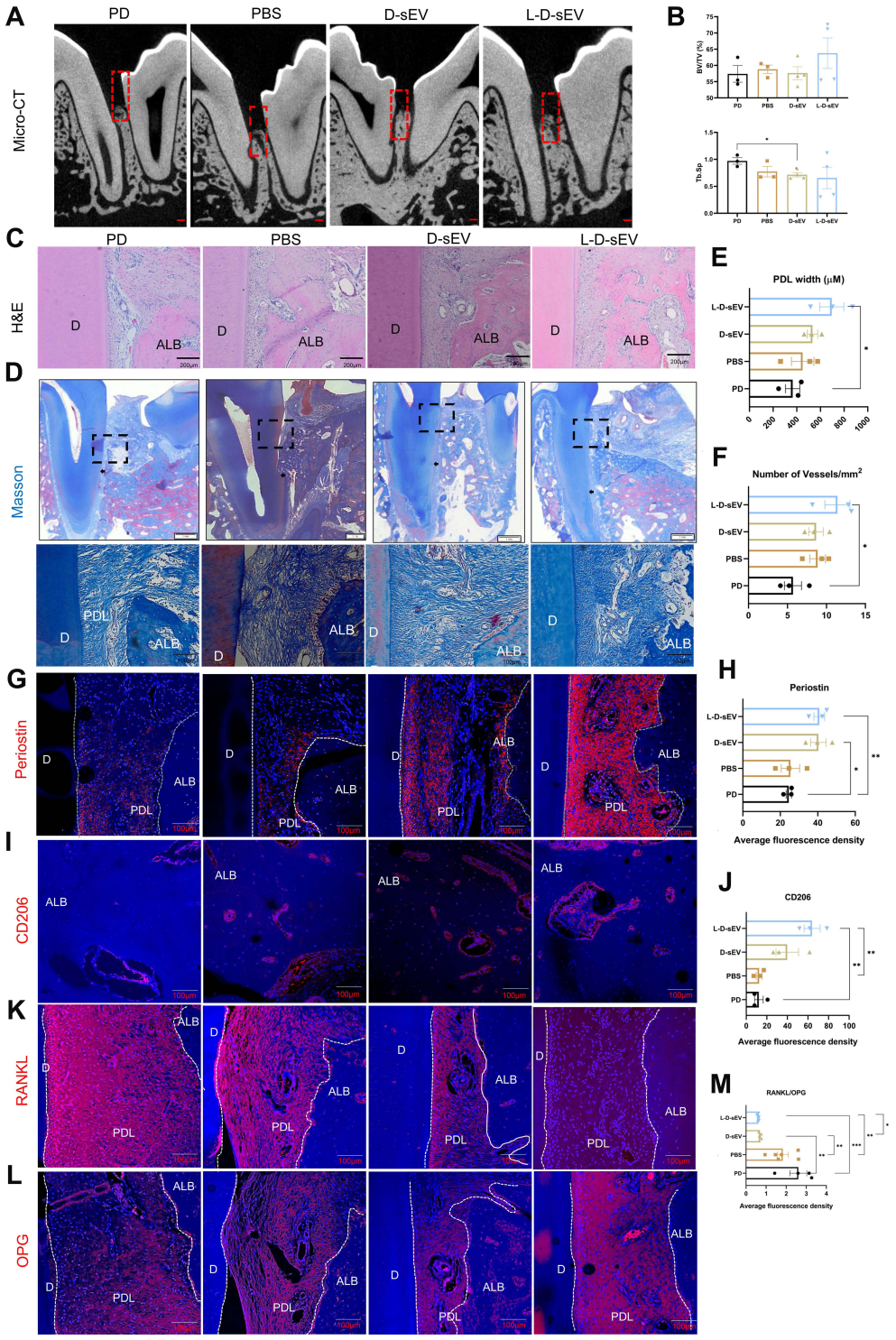

Figure 7 HA/sEV promoted periodontal regeneration in vivo. (**A**) Representative micro-CT images showing new bone formation in the PD, PBS, D-sEV, and L-D-sEV groups at 8 weeks post-injection. Scale bar: 1 mm. The red box represents the bone defect size. (**B**) The BV/TV and Tb. SP comparison. (**C**) The representative H&E stained sections. Scale bar: 200 μm. (**D**) The representative Masson stained sections. The black arrow represents Notch. (**E**) Quantitative analysis of PDL width. (**F**) The number of vessels in the PDL. (**G**) Representative images of Periostin immunofluorescence staining in PDL. Scale bar:100 μm. (**H**) Quantitative analysis of Periostin expression in PDL. (**I**) Representative images of CD206 immunofluorescence staining in ALB. Scale bar: 100 μm. (**J**) Quantitative analysis of CD206 expression in ALB. (**K**) Representative images of RANKL immunofluorescence staining in PDL. Scale bar: 100 μm. (**L**) Representative images of OPG immunofluorescence staining in PDL. Scale bar: 100 μm. (**M**) Quantitative analysis of RANKL/OPG ratio in PDL. Data are shown as the mean ± SEM for three independent experiments. *P < 0.05; **P < 0.01; ***P < 0.001.

Abbreviations: ALB, alveolar bone; D, dentin; PDL, periodontal ligament; PD, periodontitis group; HA, 0.2% hyaluronic acid gel; PBS, PBS-loaded HA; D-sEV, D-sEV-loaded HA; L-D-sEV, L-D-sEV-loaded HA.

https://doi.org/10.2147/IJN.S350869 DovePress

Table 4 Serum IgA, IgG, IgM, C3, C4, and CRP Levels in Canine

	IgA (g/L)	IgG (g/L)	IgM (g/L)	C3 (g/L)	C4 (g/L)	CRP(μg/L)
N	<0.1	1.92	1.08	<0.1	0.06	290
0 W	<0.1	2.00	1.41	<0.1	0.06	280
4 W	<0.1	1.44*	1.33	<0.1	0.06	240
8 W	<0.1	1.70**	1.13	<0.1	0.06	230

Notes: Serum immunoglobulins (IgA, IgG, IgM), complements (C3, C4), and CRP fluctuated slightly around normal levels in the following month after surgery. N, normal condition; 0 W, post-operation (1 month after experimental periodontitis induction); 4W, postoperative for 4 weeks; 8 W, postoperative for 8 weeks. Data are shown as mean. (4 W vs 0 W) *P < 0.05; (8 W vs 0 W) **P < 0.01.

microenvironment.[36,37] We proved that sEV isolated from LPS-preconditioned DFSCs was a better inducer to encourage PDLSCs to form complete periodontal tissue.

The host immune response affects the rate and severity of periodontitis.[38] A novel therapeutic strategy combined with the host-modulatory effect could increase the possibility of successfully managing periodontitis. OS has been highly associated with the onset of several inflammatory pathologies, including periodontitis and osteoporosis.[39,40] Excessive accumulation of ROS will induce DNA damage, lipid peroxidation, and protein modification, subsequently causing cellular dysfunction and tissue damage.[41,42] Appropriate removal of excess ROS is conducive to osteogenic differentiation and reduces osteoclastogenesis.[43,44] Since OS is one of the leading causes of periodontal tissue inflammation and damage,[44] antioxidant therapy has become a new treatment for periodontitis. Potentially novel therapeutic approaches to managing periodontitis rely on the use of antioxidants (eg, resveratrol, curcumin), thereby arresting the initiation and progression of periodontal disease.[45–47]

After LPS pretreatment, GSR and SOD1 were more enriched in DFCs-sEV, which can consume ROS and reduce cell oxidative damage. GSR catalyzes GSSG to GSH using NADPH as an electron donor (NADPH + H+ + GSSG → NADP+ + 2 GSH).[48] SOD1 binds to copper and zinc ions and is one of three SODs responsible for destroying free superoxide radicals in the body.[49] GSH can maintain MSCs function by reducing cell senescence and promoting cell migration, as well as by inhibiting the generation of ROS to maintain stemness and multidirectional differentiation potential.[50] The proper redox balance between ROS and antioxidants greatly contributes to the physiological well-being of cells.[51] In this study, D-sEV and L-D-sEV significantly promoted the viability of PDLSCs and macrophages in a dose- and time-dependent manner.

Studies have proven that the exposure of MSCs to LPS can increase their trophic effects and functional properties to defend against the inflammatory environment.[52,53] In this study, we found that D-sEV and L-D-sEV were selective or targeted, which could improve and guide damaged PDLSCs to restore normal physiological functions and promote tissue homeostasis, especially after LPS preconditioning. ROS-mediated JNK signaling is related to RANKL-induced osteoclastogenesis,[54] while ERK is crucial for osteoclast survival.[55,56] L-D-sEV attenuated the phosphorylation of JNK without affecting ERK, suggesting that it suppressed osteoclastogenesis but not osteoclast survival. Increasing the level of ROS in osteoclasts may promote osteoclast formation and activation.[57,58] Considering these reasons, it is most likely because GSR and SOD1 were enriched in L-D-sEV to exert antioxidant activity. The accumulation of intracellular ROS can affect MAPK/JNK signaling pathways, which can be inhibited by antioxidants to reduce ROS accumulation.[59]

On the other hand, M2 macrophages play a monitoring role in the process of bone tissue repair and regeneration, regulating the balance between osteoblasts and osteoclasts. Both D-sEV and L-D-sEV promoted M2 infiltration and polarization with lower ROS levels and higher SOD1 expression, while L-D-sEV was more effective. N-acetyl cysteine (NAC) could not impact the total number of macrophages but partly promoted M2 macrophage polarization.[60] The application of ROS scavenging material leads to the efficient polarization of M1 to M2 in the rheumatoid arthritis model.[61] It promotes healing of bacteria-infected diabetic wounds by upregulating M2 phenotype macrophages,[62] highlighting that ROS levels are critical for M2 polarization. Antioxidants or GSH status play a critical role in regulating monocyte-to-macrophage differentiation and inflammation.[63,64] L-D-sEV significantly

decreased the GSSG/GSH ratio in macrophages with an abundant GSR. Therefore, intracellular GSR and SOD1 in macrophages were significantly increased by engulfing L-D-sEV to strengthen the antioxidant capacity and reduce intracellular ROS levels. However, the SOD2 levels were not significantly changed. SOD1 is present in the cytoplasm and mitochondrial intermembrane, and SOD2 localizes to the mitochondrial matrix.[65] These results demonstrated that D-sEV and L-D-sEV play antioxidant roles mainly in the cytoplasm rather than in the mitochondria. In addition, we found that MAPK/ERK signaling was activated by L-D-sEV and mediated a more effective anti-OS function than D-sEV. According to the above results, L-D-sEV may act on PDLSCs and macrophages through antioxidant proteins under inflammatory conditions, reducing intracellular ROS levels and thereby promoting tissue repair and regeneration. Therefore, L-D-sEV could be applied as a local drug to deliver antioxidant properties in periodontitis.

However, if sEV are applied to periodontal pockets alone, the efficiency of sEV is reduced by the flow of saliva and the unclosed space of periodontal pockets. It is necessary to construct an excellent delivery system to maintain the sustained therapeutic effect of sEV. Actually, in the process of clinical transformation of stem cells and their derivatives, the components of biological agents should be as clear as possible, and their safety and effectiveness should be guaranteed. Gengigel® contains 0.2% hyaluronic acid (HA) gel that provides stability and elasticity to tissues and delays penetration of viruses and bacteria.[66] This experiment confirmed that a mixture of HA and sEV in an appropriate ratio can still maintain the injectability and release 80% of sEV slowly within one week without affecting the biological functions of sEV. Therefore, HA is a convenient, safe, and effective scaffold material that is suitable for auxiliary sEV in clinical applications.

In canine critical-sized periodontal defects with periodontitis, we found that xenogeneic DFC-sEV transplantation had good biological safety and did not cause obvious immune rejection. Furthermore, micro-CT and histological analysis indicated that D-sEV had therapeutic effects on periodontitis with more new bone and PDL formation via elevation of M2 infiltration and inhibition of RANKL/OPG, and L-D-sEV further enhanced the effects. Remarkably, antioxidant activity was provided for the scaffold and positively influenced the bone repaired microenvironment.[67] The influence of sEV on a variety of cells in periodontal tissue makes the microenvironment of periodontal tissue change from "killing and destroying" to "repairing and healing", thereby preserving more original periodontium and promoting regeneration of the damaged periodontium. MSCs-derived sEV can promote the proliferation, migration, and differentiation of target cells in a dose-dependent and saturable manner.[68] Clarifying the dosage and frequency of sEV application in periodontal tissue regeneration is crucial for its clinical application. According to the release rate of sEV, the administration frequency was once a week for four consecutive weeks. In animal models, if a defect area can be completely enclosed, such as a joint cavity,[69] subcutaneous,[70] bone defect,[71] etc., a single administration will be chosen. However, administration to the periodontal pocket communicating with the Oral cavity will cause a loss, and multiple administrations are needed to improve the treatment effect.

Compared with MSCs transplantation, the use of MSC-derived exosomes/microvesicles in human patients has several potential advantages, such as avoiding the transfer of cells that have mutated or damaged DNA, being small and circulating readily, and achieving a higher "dose" that circulates.[72] Although the periodontal ligament and alveolar bone were successfully regenerated in canine, several problems remain to be solved. The sEV/HA strategy must be investigated further in rhesus monkeys and optimize the application project to make it work more effective. Additionally, standardized operation procedures and a safety evaluation system should be established serially and systematically to guarantee the feasibility of the clinical application of sEV.

Conclusions

In summary, LPS-preconditioned D-sEV possessed an apparent advantage for alveolar bone loss inhibition and regeneration in canines with experimental periodontitis, possibly based on ROS/MAPK-mediated antioxidant effects. The HA/sEV injectable loading system had the advantages of good injectability, good sustained-release effect, and anti-inflammatory properties, which were safe and beneficial to clinical application, and it could be effectively used as an auxiliary method for the treatment of periodontitis.

Abbreviations

DFSCs, dental follicle stem cells; PDLSCs, periodontal ligament stem cells; LPS, lipopolysaccharide; sEV, small extracellular vesicles; D-sEV, dental follicle stem cells-derived small extracellular vesicles; L-D-sEV, LPS-preconditioned dental follicle stem cells-derived small extracellular vesicles; TEM, transmission electron microscopy; NTA, nanoparticle tracking analysis; HSP70, heat shock protein 70; HA, 0.2% hyaluronic acid gel; CCK-8, cell counting kit-8; M0, macrophage; M2, type 2 macrophage; OD, optical density; PEG, polyethylene glycol; RANKL, NF-kB receptor activator; OPG, osteogenic protective protein; ROS, reactive oxygen species; OS, oxidative stress; MAPK, mitogen-activated protein kinase; JNK, Jun amino-terminal kinases; ERK, extracellular signal-related kinases; GSR, Glutathione reductase; PDIA6, Protein disulfide-isomerase A6; PPIA, Peptidyl-prolyl cis-trans isomerase A; ME1, NADP-dependent malic enzyme; DCXR, L-xylulose reductase; UCHL1, Ubiquitin carboxyl-terminal hydrolase isozyme L1; FH, Fumarate hydratase; CTSA, Lysosomal protective protein; PTK7, Inactive tyrosine-protein kinase 7; LTF, Lactotransferrin; MAP2K1, Dual specificity mitogen-activated protein kinase kinase 1; P4HA2, Prolyl 4-hydroxylase subunit alpha-2; SOD1, Superoxide dismutase [Cu-Zn] 1; MET, Hepatocyte growth factor receptor; CKB, Creatine kinase B-type; RPS3, 40S ribosomal protein S3; PPT1, Palmitoyl-protein thioesterase 1; EPHA4, Ephrin type-A receptor 4; PTGES3, Prostaglandin E synthase 3; PPM1A, Protein phosphatase 1A; EIF2S3B, Eukaryotic translation initiation factor 2 subunit 3B; GSSG, reduction of oxidized glutathione; GSH, reduced glutathione; SOD2, Superoxide dismutase 2;GO, Gene ontology; DEPs, differentially expressed proteins; PPI, protein–protein interaction; KEGG, Kyoto Encyclopedia of Genes and Genomes; CRP, C-reactive protein; PDL, periodontal ligament; BV/TV, bone volume/total volume; Tb. Sp, trabecular separation; H&E, hematoxylin-eosin.

Data Sharing Statement

All data generated or analyzed during this study are included in this published article.

Ethics Approval and Informed Consent

All animal experiments were performed according to protocols approved by the Institutional Animal Care and Use Committee (IACUC) at Sichuan University. This study was reviewed and approved by the Committee of Ethics of West China Hospital of Stomatology, Sichuan University (NO. WCHSIRB-D-2021-470 and WCHSIRB-D-2021-450).

Consent for Publication

The manuscript does not contain individual person's data. The consent for publication does not apply.

Funding

This work was supported by the National Key Research and Development Program of China (Grant number 2017YFA0104800) and the Key Research and Development Program of Sichuan Province (Grant number 2020YFS0175).

Disclosure

The authors report no potential conflicts of interest in this work.

References

1. Page RC, Kornman KS. The pathogenesis of human periodontitis: an introduction. *Periodontol*. 1997;14:9–11. doi:10.1111/j.1600-0757.1997.tb00189.x
2. Chávarry NG, Vettore MV, Sansone C, Sheiham A. The relationship between diabetes mellitus and destructive periodontal disease: a meta-analysis. *Oral Health Prev Dent*. 2009;7(2):107–127.
3. Ramírez JH, Parra B, Gutierrez S, et al. Biomarkers of cardiovascular disease are increased in untreated chronic periodontitis: a case control study. *Aust Dent J*. 2014;59(1):29–36. doi:10.1111/adj.12139
4. Ide M, Harris M, Stevens A, et al. Periodontitis and Cognitive Decline in Alzheimer's Disease. *PLoS One*. 2016;11(3):e0151081. doi:10.1371/journal.pone.0151081
5. El Moshy S, Radwan IA, Rady D, et al. Dental stem cell-derived secretome/conditioned medium: the future for regenerative therapeutic applications. *Stem Cells Int*. 2020;2020:7593402. doi:10.1155/2020/7593402

6. Bi R, Lyu P, Song Y, et al. Function of dental follicle progenitor/stem cells and their potential in regenerative medicine: from mechanisms to applications. *Biomolecules*. 2021;11(7):997. doi:10.3390/biom11070997
7. Meirelles Lda S, Fontes AM, Covas DT, Caplan AI. Mechanisms involved in the therapeutic properties of mesenchymal stem cells. *Cytokine Growth Factor Rev*. 2009;20(5–6):419–427. doi:10.1016/j.cytogfr.2009.10.002
8. Weiss ARR, Dahlke MH. Immunomodulation by Mesenchymal Stem Cells (MSCs): mechanisms of Action of Living, Apoptotic, and Dead MSCs. *Front Immunol*. 2019;10:1191. doi:10.3389/fimmu.2019.01191
9. Luan X, Zhou X, Trombetta-eSilva J, et al. MicroRNAs and Periodontal Homeostasis. *J Dent Res*. 2017;96(5):491–500. doi:10.1177/0022034516685711
10. Garlet GP. Destructive and protective roles of cytokines in periodontitis: a reappraisal from host defense and tissue destruction viewpoints. *J Dent Res*. 2010;89(12):1349–1363. doi:10.1177/0022034510376402
11. Cardoso EM, Reis C, Manzanares-Céspedes MC. Chronic periodontitis, inflammatory cytokines, and interrelationship with other chronic diseases. *Postgrad Med*. 2018;130(1):98–104. doi:10.1080/00325481.2018.1396876
12. Konopka L, Pietrzak A, Brzezińska-Błaszczyk E. Effect of scaling and root planing on interleukin-1β, interleukin-8 and MMP-8 levels in gingival crevicular fluid from chronic periodontitis patients. *J Periodontal Res*. 2012;47(6):681–688. doi:10.1111/j.1600-0765.2012.01480.x
13. Katsuda T, Kosaka N, Takeshita F, Ochiya T. The therapeutic potential of mesenchymal stem cell-derived extracellular vesicles. *Proteomics*. 2013;13(10–11):1637–1653. doi:10.1002/pmic.201200373
14. Song Y, Dou H, Li X, et al. Exosomal miR-146a Contributes to the Enhanced Therapeutic Efficacy of Interleukin-1β-Primed Mesenchymal Stem Cells Against Sepsis. *Stem Cells*. 2017;35(5):1208–1221. doi:10.1002/stem.2564
15. Kurte M, Vega-Letter AM, Luz-Crawford P, et al. Time-dependent LPS exposure commands MSC immunoplasticity through TLR4 activation leading to opposite therapeutic outcome in EAE. *Stem Cell Res Ther*. 2020;11(1):416. doi:10.1186/s13287-020-01840-2
16. Kim WJ, Park SY, Kim OS, Park HS, Jung JY. Autophagy upregulates inflammatory cytokines in gingival tissue of patients with periodontitis and lipopolysaccharide-stimulated human gingival fibroblasts. *J Periodontol Epub*. 2021. doi:10.1002/JPER.21-0178
17. Lee MK, Ide M, Coward PY, Wilson RF. Effect of ultrasonic debridement using a chlorhexidine irrigant on circulating levels of lipopolysaccharides and interleukin-6. *J Clin Periodontol*. 2008;35(5):415–419. doi:10.1111/j.1600-051X.2008.01221.x
18. Shi W, Guo S, Liu L, et al. Small Extracellular Vesicles from Lipopolysaccharide-Preconditioned Dental Follicle Cells Promote Periodontal Regeneration in an Inflammatory Microenvironment. *ACS Biomater Sci Eng*. 2020;6(10):5797–5810. doi:10.1021/acsbiomaterials.0c00882
19. Greening DW, Gopal SK, Xu R, Simpson RJ, Chen W. Exosomes and their roles in immune regulation and cancer. *Semin Cell Dev Biol*. 2015;40:72–81. doi:10.1016/j.semcdb.2015.02.009
20. He X, Dong Z, Cao Y, et al. MSC-Derived Exosome Promotes M2 Polarization and Enhances Cutaneous Wound Healing. *Stem Cells Int*. 2019;2019:7132708. doi:10.1155/2019/7132708
21. Maia J, Caja S, Strano Moraes MC, Couto N, Costa-Silva B. Exosome-Based Cell–Cell Communication in the Tumor Microenvironment. *Front Cell Dev Biol*. 2018;6:18. doi:10.3389/fcell.2018.00018
22. Javeed N, Mukhopadhyay D. Exosomes and their role in the micro/macroenvironment: a comprehensive review. *J Biomed Res*. 2017;31(5):386–394. doi:10.7555/JBR.30.20150162
23. Eldh M, Ekstrom K, Valadi H, et al. Exosomes communicate protective messages during oxidative stress; possible role of exosomal shuttle RNA. *PLoS One*. 2010;5(12):e15353. doi:10.1371/journal.pone.0015353
24. Guo S, Guo W, Ding Y, et al. Comparative study of human dental follicle cell sheets and periodontal ligament cell sheets for periodontal tissue regeneration. *Cell Transplant*. 2013;22(6):1061–1073. doi:10.3727/096368912X656036
25. Yang H, Li J, Hu Y, et al. Treated dentin matrix particles combined with dental follicle cell sheet stimulate periodontal regeneration. *Dent Mater*. 2019;35(9):1238–1253. doi:10.1016/j.dental.2019.05.016
26. Guo S, Kang J, Ji B, et al. Periodontal-Derived Mesenchymal Cell Sheets Promote Periodontal Regeneration in Inflammatory Microenvironment. *Tissue Eng Part A*. 2017;23(13–14):585–596. doi:10.1089/ten.tea.2016.0334
27. Van Tuyl LH, Voskuyl AE, Boers M, et al. Baseline RANKL:OPG ratio and markers of bone and cartilage degradation predict annual radiological progression over 11 years in rheumatoid arthritis. *Ann Rheum Dis*. 2010;69(9):1623–1628. doi:10.1136/ard.2009.121764
28. Chio IIC, Tuveson DA. ROS in Cancer: the Burning Question. *Trends Mol Med*. 2017;23(5):411–429. doi:10.1016/j.molmed.2017.03.004
29. Lee K, Seo I, Choi MH, Jeong D. Roles of Mitogen-Activated Protein Kinases in Osteoclast Biology. *Int J Mol Sci*. 2018;19(10):3004. doi:10.3390/ijms19103004
30. Stein M, Keshav S, Harris N, Gordon S. Interleukin 4 potently enhances murine macrophage mannose receptor activity: a marker of alternative immunologic macrophage activation. *J Exp Med*. 1992;176(1):287–292. doi:10.1084/jem.176.1.287
31. Martinez FO, Gordon S. The M1 and M2 paradigm of macrophage activation: time for reassessment. *F1000Prime Rep*. 2014;6:13. doi:10.12703/P6-13
32. Yin C, Zhao Q, Li W, et al. Biomimetic anti-inflammatory nanocapsule serves as a cytokine blocker and M2 polarization inducer for bone tissue repair. *Acta Biomater*. 2020;102:416–426. doi:10.1016/j.actbio.2019.11.025
33. Vašíček O, Lojek A, Číž M. Serotonin and its metabolites reduce oxidative stress in murine RAW264.7 macrophages and prevent inflammation. *J Physiol Biochem*. 2020;76(1):49–60. doi:10.1007/s13105-019-00714-3
34. Zhang Y, Choksi S, Chen K, Pobezinskaya Y, Linnoila I, Liu ZG. ROS play a critical role in the differentiation of alternatively activated macrophages and the occurrence of tumor-associated macrophages. *Cell Res*. 2013;23(7):898–914. doi:10.1038/cr.2013.75
35. Damiano S, Petrozziello T, Ucci V, Amente S, Santillo M, Mondola P. Cu-Zn superoxide dismutase activates muscarinic acetylcholine M1 receptor pathway in neuroblastoma cells. *Mol Cell Neurosci*. 2013;52:31–37. doi:10.1016/j.mcn.2012.11.001
36. Munir S, Basu A, Maity P, et al. TLR4-dependent shaping of the wound site by MSCs accelerates wound healing. *EMBO Rep*. 2020;21(5):e48777. doi:10.15252/embr.201948777
37. Shah SA, Khan M, Jo M-H, Jo MG, Amin FU, Kim MO. Melatonin Stimulates the SIRT1/Nrf2 Signaling Pathway Counteracting Lipopolysaccharide (LPS)-Induced Oxidative Stress to Rescue Postnatal Rat Brain. *CNS Neurosci Ther*. 2017;23(1):33–44. doi:10.1111/cns.12588
38. Lamont RJ, Koo H, Hajishengallis G. The oral microbiota: dynamic communities and host interactions. *Nat Rev Microbiol*. 2018;16(12):745–759. doi:10.1038/s41579-018-0089-x

39. Wang Y, Andrukhov O, Rausch-Fan X. Oxidative Stress and Antioxidant System in Periodontitis. *Front Physiol*. 2017;8:910. doi:10.3389/fphys.2017.00910
40. Wilson C. Bone: oxidative stress and osteoporosis. *Nat Rev Endocrinol*. 2014;10(1):3.doi:10.1038/nrendo.2013.225
41. Zhao MJ, Yuan S, Zi H, Gu JM, Fang C, Zeng XT. Oxidative Stress Links Aging-Associated Cardiovascular Diseases and Prostatic Diseases. *Oxid Med Cell Longev*. 2021;2021:5896136. doi:10.1155/2021/5896136
42. Jomova K, Valko M. Advances in metal-induced oxidative stress and human disease. *Toxicology*. 2011;283(2–3):65–87. doi:10.1016/j.tox.2011.03.001
43. Qiu X, Yu Y, Liu H, et al. Remodeling the periodontitis microenvironment for osteogenesis by using a reactive oxygen species-cleavable nanoplatform. *Acta Biomater*. 2021;135:593–605. doi:10.1016/j.actbio.2021.08.009
44. Lee KE, Mo S, Lee HS, et al. Deferoxamine Reduces Inflammation and Osteoclastogenesis in Avulsed Teeth. *Int J Mol Sci*. 2021;22(15):8225. doi:10.3390/ijms22158225
45. Corrêa MG, Absy S, Tenenbaum H, et al. Resveratrol attenuates oxidative stress during experimental periodontitis in rats exposed to cigarette smoke inhalation. *J Periodontal Res*. 2019;54(3):225–232. doi:10.1111/jre.12622
46. Bakır B, Yetkin AZ, Büyükbayram Hİ, et al. Effect of curcumin on systemic T helper 17 cell response; gingival expressions of interleukin-17 and retinoic acid receptor-related orphan receptor γt; and alveolar bone loss in experimental periodontitis. *J Periodontol*. 2016;87(11):e183–e191. doi:10.1902/jop.2016.150722
47. Elavarasu S, Suthanthiran T, Thangavelu A, Alex S, Palanisamy VK, Kumar TS. Evaluation of superoxide dismutase levels in local drug delivery system containing 0.2% curcumin strip as an adjunct to scaling and root planing in chronic periodontitis: a clinical and biochemical study. *J Pharm Bioallied Sci*. 2016;8(Suppl 1):S48–S52. doi:10.4103/0975-7406.191967
48. Hoffmann C, Dietrich M, Herrmann AK, Schacht T, Albrecht P, Methner A. Dimethyl Fumarate Induces Glutathione Recycling by Upregulation of Glutathione Reductase. *Oxid Med Cell Longev*. 2017;2017:6093903. doi:10.1155/2017/6093903
49. Hwang J, Jin J, Jeon S, et al. SOD1 suppresses pro-inflammatory immune responses by protecting against oxidative stress in colitis. *Redox Bio*. 2020;37:101760. doi:10.1016/j.redox.2020.101760
50. Liao N, Shi Y, Zhang C, et al. Antioxidants inhibit cell senescence and preserve stemness of adipose tissue-derived stem cells by reducing ROS generation during long-term in vitro expansion. *Stem Cell Res Ther*. 2019;10(1):306. doi:10.1186/s13287-019-1404-9
51. Climent M, Viggiani G, Chen YW, Coulis G, Castaldi A. MicroRNA and ROS Crosstalk in Cardiac and Pulmonary Diseases. *Int J Mol Sci*. 2020;21(12):4370. doi:10.3390/ijms21124370
52. Yao Y, Zhang F, Wang L, et al. Lipopolysaccharide preconditioning enhances the efficacy of mesenchymal stem cells transplantation in a rat model of acute myocardial infarction. *J Biomed Sci*. 2009;16(1):74. doi:10.1186/1423-0127-16-74
53. Wang ZJ, Zhang FM, Wang LS, Yao YW, Zhao Q, Gao X. Lipopolysaccharides can protect mesenchymal stem cells (MSCs) from oxidative stress-induced apoptosis and enhance proliferation of MSCs via Toll-like receptor (TLR)-4 and PI3K/Akt. *Cell Biol Int*. 2009;33(6):665–674. doi:10.1016/j.cellbi.2009.03.006
54. Chen K, Qiu P, Yuan Y, et al. Pseurotin An Inhibits Osteoclastogenesis and Prevents Ovariectomized-Induced Bone Loss by Suppressing Reactive Oxygen Species. *Theranostics*. 2019;9(6):1634–1650. doi:10.7150/thno.30206
55. Davis RJ. Signal transduction by the JNK group of MAP kinases. *Cell*. 2000;103(2):239–252. doi:10.1016/S0092-8674(00)00116-1
56. Lee SE, Chung WJ, Kwak HB, et al. Tumor necrosis factor-alpha supports the survival of osteoclasts through the activation of Akt and ERK. *J Biol Chem*. 2001;276(52):49343–49349. doi:10.1074/jbc.M103642200
57. Ha H, Kwak HB, Lee SW, et al. Reactive oxygen species mediate RANK signaling in osteoclasts. *Exp Cell Res*. 2004;301(2):119–127. doi:10.1016/j.yexcr.2004.07.035
58. Lee NK, Choi YG, Baik JY, et al. A crucial role for reactive oxygen species in RANKL-induced osteoclast differentiation. *Blood*. 2005;106(3):852–859. doi:10.1182/blood-2004-09-3662
59. Yang G, Chang CC, Yang Y, et al. Resveratrol Alleviates Rheumatoid Arthritis via Reducing ROS and Inflammation, Inhibiting MAPK Signaling Pathways, and Suppressing Angiogenesis. *J Agric Food Chem*. 2018;66(49):12953–12960. doi:10.1021/acs.jafc.8b05047
60. Zhu QY, Tai S, Tang L, et al. N-acetyl cysteine ameliorates aortic fibrosis by promoting M2 macrophage polarization in aging mice. *Redox Rep*. 2021;26(1):170–175. doi:10.1080/13510002.2021.1976568
61. Nakao Y, Fukuda T, Zhang Q, et al. Exosomes from TNF-α-treated human gingiva-derived MSCs enhance M2 macrophage polarization and inhibit periodontal bone loss. *Acta Biomater*. 2021;122:306–324. doi:10.1016/j.actbio.2020.12.046
62. Kim J, Kim HY, Song SY, et al. Synergistic Oxygen Generation and Reactive Oxygen Species Scavenging by Manganese Ferrite/Ceria Codecorated Nanoparticles for Rheumatoid Arthritis Treatment. *ACS Nano*. 2019;13(3):3206–3217. doi:10.1021/acsnano.8b08785
63. Vasamsetti SB, Karnewar S, Gopoju R, et al. Resveratrol attenuates monocyte-to-macrophage differentiation and associated inflammation via modulation of intracellular GSH homeostasis: relevance in atherosclerosis. *Free Radic Biol Med*. 2016;96:392–405. doi:10.1016/j.freeradbiomed.2016.05.003
64. Roberts CP, Murphy AA, Santanam N, Parthasarathy S. Regulation of monocyte to macrophage differentiation by antiglucocorticoids and antioxidants. *Am J Obstet Gynecol*. 1998;179(2):354–362. doi:10.1016/S0002-9378(98)70364-3
65. Okado-Matsumoto A, Fridovich I. Subcellular distribution of superoxide dismutases (SOD) in rat Liver. *J Biol Chem*. 2001;276(42):38388–38393. doi:10.1074/jbc.M105395200
66. Gupta S, Kediege SD, Gupta A, Jain K. Evaluation of Gengigel® Application in the Management of Furcation with Coronally Advanced Flap through Surgical Re-Entry-A Split Mouth Clinical Study. *J Clin Diagn Res*. 2017;11(1):ZC27–ZC32. doi:10.7860/JCDR/2017/21938.9169
67. Forte L, Torricelli P, Boanini E, Rubini K, Fini M, Bigi A. Quercetin and alendronate multifunctionalized materials as tools to hinder oxidative stress damage. *J Biomed Mater Res A*. 2017;105(12):3293–3303. doi:10.1002/jbm.a.36192
68. Huang CC, Narayanan R, Alapati S, Ravindran S. Exosomes as biomimetic tools for stem cell differentiation: applications in dental pulp tissue regeneration. *Biomaterials*. 2016;1:111,103–115. doi:10.1016/j.biomaterials.2016.09.029
69. Zhang S, Chuah SJ, Lai RC, Hui JHP, Lim SK, Toh WS. MSC exosomes mediate cartilage repair by enhancing proliferation, attenuating apoptosis and modulating immune reactivity. *Biomaterials*. 2018;156:16–27. doi:10.1016/j.biomaterials.2017.11.028
70. Wang B, Wang J, Shao J, et al. A tunable and injectable local drug delivery system for personalized periodontal application. *J Control Release*. 2020;324:134–145. doi:10.1016/j.jconrel.2020.05.004

71. Chew JRJ, Chuah SJ, Teo KYW, et al. Mesenchymal stem cell exosomes enhance periodontal ligament cell functions and promote periodontal regeneration. *Acta Biomater*. 2019;89:252–264. doi:10.1016/j.actbio.2019.03.021
72. Phinney DG, Pittenger MF. Concise Review: MSC-Derived Exosomes for Cell-Free Therapy. *Stem Cells*. 2017;35(4):851–858. doi:10.1002/stem.2575